

Conf 921129-9-
Rev. 3/93

THE PUMPING OF HYDROGEN AND HELIUM BY SPUTTER-ION PUMPS*

K.M. Welch, D.J. Pate, and R.J. Todd
RHIC Project, BNL, Upton, New York 11973.

RECEIVED
MAY 06 1993
OSTI

ABSTRACT

The pumping of hydrogen in diode and triode sputter-ion pumps is discussed. The type of cathode material used in these pumps is shown to have a significant impact on the effectiveness with which hydrogen is pumped. Examples of this include data for pumps with aluminum and titanium-alloy cathodes. Diode pumps with aluminum cathodes are shown to be no more effective in the pumping of hydrogen than in the pumping of helium. The use of titanium or titanium alloy anodes is also shown to measurably impact on the speed of these pumps at very low pressures. This stems from the fact that hydrogen is $\times 10^6$ more soluble in titanium than in stainless steel. Hydrogen becomes resident in the anodes because of fast neutral burial. Lastly, quantitative data are given for the He speeds and capacities of both noble and conventional diode and triode pumps. The effectiveness of various pump regeneration procedures, subsequent to the pumping of He, is reported. These included bakeout and N_2 glow discharge cleaning. The comparative desorption of He with the subsequent pumping of N_2 is reported on. The N_2 speed of these pumps was used as the benchmark for defining the *size* of the pumps vs. their respective He speeds.

*Work supported in part by the U.S. Department of Energy.

MASTER

DISTRIBUTION OF THIS DOCUMENT IS UNLIMITED 

INTRODUCTION

The objective of the Relativistic Heavy Ion Collider (RHIC) project is to do physics research involving the collisions of highly relativistic particle beams. The RHIC machine, described elsewhere and presently under construction,⁽¹⁾ must store two counter-rotating particle beams for periods of greater than ten hours. Colliding beams may comprise protons, gold ions (*i.e.*, Au^{+79}), or a variety of heavy ions, colliding with each other or protons.

First, the intensity, and thus usefulness, of the particle beams is diminished when the stored particles are lost from their contrived orbits either due to charge exchange processes or through nuclear scattering with background gas. Secondly, particle beam collisions with gas in regions near the experimental detectors cause background *noise* in these detectors, and are therefore undesirable. For these and other reasons, a low operating pressure in the RHIC is very important. The RHIC, illustrated in Fig. 1, comprises two interweaving rings ~3.8 km in circumference.

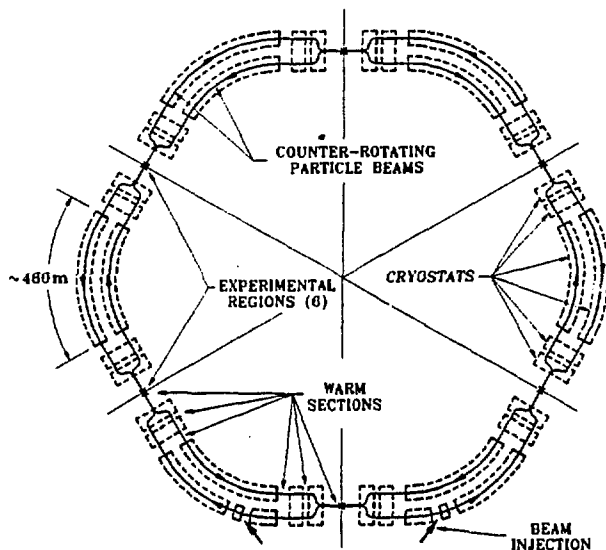


Figure 1. The Brookhaven Relativistic Heavy Ion Collider.

About seventeen percent of the life of each beam is spent in *warm*, RT (*i.e.*, room temperature) sections of the rings; the remainder is spent in beam pipe operating at a temperature of $\sim 4.2^\circ\text{K}$ (*i.e.*, the *cold-bore*). An average total pressure of $\leq 5 \times 10^{-10}$ Torr is required in the warm sections, the gases comprising 90% H_2 , 5% CO and 5% CH_4 . However, the pressure specification for beam components such as kickers, septum and RT rf cavities is $\leq 2 \times 10^{-9}$ Torr, in the same gas species proportions. The requirement for the average total pressure of the cold-bore is $\leq 10^{-11}$ Torr, comprising exclusively H_2 and He . Maintenance of the above pressures assure adequate beam life-times and acceptable beam-emittance growth rates.

THE NEED FOR HELIUM PUMPING

The RHIC cold-bore comprises seamless, austenitic stainless steel (*i.e.*, stn. stl.) tubes, which extend beyond the end-plates of the superconducting magnets, to which they are welded. The magnets, in turn, are housed within vacuum cryostats. The UHV cold-bore is interconnected between magnets with formed stn. stl. bellows. Therefore, the only means whereby He can leak into the cold-bore UHV system is: *i*) from the magnet cold-mass and through metallurgical flaws in the seamless pipe; *ii*) because of possible damage caused during the welding of the beam pipe to the magnet end-plates; or, *iii*) from the circumstance of gaseous He, in the cryostat, leaking through a catastrophic failure in the UHV interconnecting piping or bellows.

We initially planned to pump the cold-bore sections of the RHIC using small sputter-ion pumps (*i.e.*, SIPs). These pumps were to be located outside of the magnet cryostats and be coupled to the cold-bore through stn. stl. hoses. Concerns about the use of SIPs in this application served as the motivation for quantifying the helium capacities of the various types of pumps.

SPUTTER-ION PUMP CONFIGURATIONS

There are three types of SIP configurations: *i*) the conventional or *standard* diode pump; *ii*) the *noble* diode pump; and, *iii*) the *triode* pump. The variety of presently available commercial SIPs and their pumping mechanisms are discussed in detail elsewhere.⁽²⁾ In brief, the configuration of single-cell triode and diode SIPs is shown in Fig. 2. The cathodes are customarily made of some chemically active material. Gas is ionized in the hollow, Penning discharge *cell* by a swirling cloud of high energy electrons. These electrons are trapped within the cells by orthogonal electric and magnetic fields. Gas ions bombard and sputter the chemically active cathode material. The lighter gases, such as He and H₂, do not effectively sputter the cathodes. Chemically active gases (*i.e.*, active with the cathode materials) are pumped by chemisorption and the inert gases by physisorption.

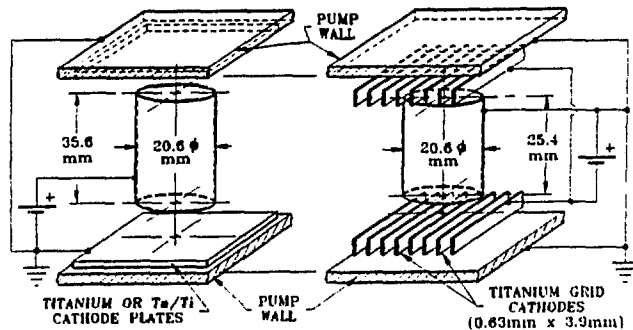


Figure 2. Configurations of single-cell diode and triode sputter-ion pumps.

The primary physisorption mechanism is the burial of high energy neutral gas atoms or molecules. If an energetic gas ion strikes a metal surface, there is a probability that it will *steal* an electron from the surface, and rebound as an energetic neutral atom. These energetic neutrals are reflected back from the cathodes and buried as neutrals in all pump surfaces. If a gas is not chemically active with the cathode material, it can only be pumped by burial as a high energy neutral or gas ion.

The principle difference between standard diodes and noble diodes is exclusively in the selection of cathode material. In the case of the noble diode, sometimes called the DI[®] pump, one cathode comprises Ti and the second Ta. The Ta atoms in the one cathode serve as a high-inertia crystal lattice for the reflection and burial of neutrals in other surfaces. In the conventional diode, both cathodes comprise Ti. The diode anode is operated at a positive voltage with respect to ground and the cathodes at ground potential.

The triode anode - the word *triode* is a misnomer - is operated at ground potential, and the cathodes at a negative potential with respect to ground. The cathodes of triode pumps are somewhat transparent to high energy neutrals created by charge exchange processes at these surfaces. Some of the gas ions which are created in the discharge cell pick up an electron on impingement with the cathodes, and pass on through the transparent grids as high energy neutrals. These neutrals are implanted in the walls of the pump, immune to subsequent sputter-desorption.

PUMP CAPACITY

Much work has been done in the last thirty years in measuring speeds and capacities of SIPs for the inert gases of ≥ 20 amu and the chemically active gases. A detailed review of this work is given elsewhere.⁽²⁾ However, a paucity of data exists on He capacities of these pumps.⁽³⁻⁶⁾ In fact, a universal definition of the meaning of *capacity* does not exist.

By definition, at the *base pressure* of a pump, the speed of the pump is zero. We herein define the *capacity* of a pump as the change in base pressure of a pump stemming from pumping a specified amount of a particular gas. We herein arbitrarily define the *He base pressure*, P_b , as that pressure achieved by the pump ≥ 20 hours subsequent to the removal of the He leak. Because of the very slow decay in pressure on removal of the He leak, this proves to be a very liberal definition of *base pressure*.

The speed of a pump, S , as a function of pump operating pressure, P_0 , is given by:

$$S = S_{\max} (1 - (P_b(\int Q dt) / P_0)), \quad (1)$$

where, S_{\max} = the maximum pump speed in ℓ/sec ,

$P_b(\int Q dt)$ = the base pressure of the pump, in Torr,
as a function of Torr- ℓ of gas pumped,

Q = the rate of gas introduction, Torr- ℓ/sec ,

and, $\int Q dt$ = the amount of gas pumped in time t , Torr- ℓ .

Actually, the idealized speed, S_{max} , given by (1), does not take into account I/P considerations of the SIP,⁽⁷⁾ nor does it address inherent high pressure limiting mechanisms. However, using this simple model, it is evident that when $P_b = P_0$, the speed of the pump is zero. For many gases, a capture pump base pressure, P_b , is a function of $\int Q dt$. This is observed when pumping all of the noble gases with SIPs. If P_b is a function $\int Q dt$ for a given gas, it is meaningless to make a statement about the speed for this gas, S , in the absence of a statement about the amount of the specific gas pumped up to that time. This effect is illustrated in Fig. 3. In this figure pump speed as a function of pressure, $S(P)$, is depicted for three cases: $\int Q_1 dt < \int Q_2 dt < \int Q_3 dt$. As a consequence of increasing base pressure, with successively greater amounts of pumped gas, the speed of the pump is seen to diminish at a fixed pressure. For example, as shown in Fig. 3, after pumping $\int Q_1 dt$ amount of gas, at a pressure P_2 , the speed of the pump is seen to be $\sim 0.75 S_{max}$. On the other hand, after pumping $\int Q_2 dt$ amount of gas the speed is zero at P_2 , as P_2 is now, due to capacity effects, the pump base pressure, P_b .

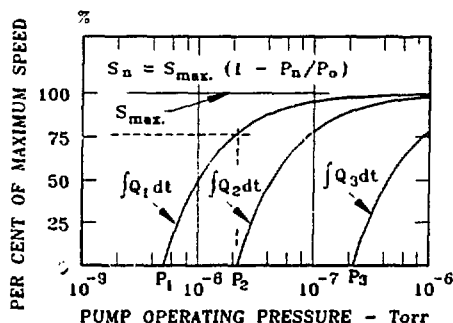


Figure 3. Increases in a capture pump's base pressure (i.e., P_1 , P_2 & P_3) as a consequence of pumping increasing amounts of a particular gas (i.e., $\int Q_1 dt$, $\int Q_2 dt$ & $\int Q_3 dt$ respectively)

EXPERIMENTAL APPARATUS

The apparatus used in making these quantitative He measurements, shown in Fig. 4, was a modified Fischer-Mommsen Dome.⁽⁸⁾ This dome, sometimes referred to as a CERN dome, was used to make speed determinations as a function of the amount of He pumped. A NIST⁽⁹⁾ traceable capacitance manometer, appending a NIST traceable known volume, was used to measure gas throughput and the total amount of He introduced into the system through an all-metal, variable leak appending the dome. A long stn. stl. capillary was used to attached this throughput measuring apparatus to the variable leak. This permitted thermal decoupling of the apparatus from the dome during the 48 hour, 250°C dome and pump bakeouts.

A calibrated quadrupole residual gas analyzer (i.e., QRG) and calibrated Bayard-Alpert gauge (i.e., BAG) were used to measure the pressure differences across the dome aperture. Agreement

to within $\pm 10\%$ existed between measured pump speeds and pump inlet pressures and $V_1 dP_1/dt$ results of the gas introduction system, where V_1 is the volume of the gas inlet system and P_1 the pressure measured with the capacitance manometer.

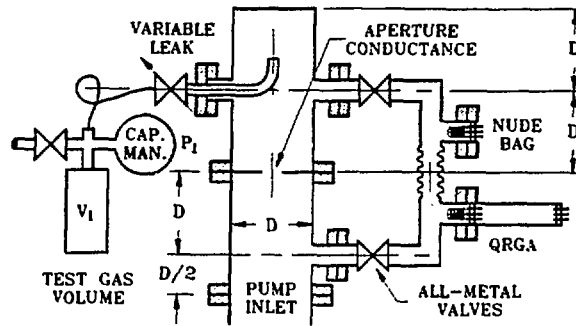


Figure 4. Modified Fischer-Mommsen speed measuring dome.

One advantage of the modified CERN dome configuration is that the same gauge can be used to measure the pressure on both sides of the fixed aperture. For example, assume that the dome gauge is in error by a factor k , so that the absolute pressure is $P_{abs.} = k P_i$, where P_i is the indicated pressure. Then, the speed of the pump is given by:

$$S = C_a (kP_{iH} - kP_{iL}) \div kP_{iL} = C_a (P_{iH} - P_{iL}) \div P_{iL}, \quad (2)$$

where, C_a = the aperture conductance in $l/sec.$,
 P_{iH} = the *high* indicated pressure, in Torr,
and, P_{iL} = the *low* indicated pressure, in Torr.

As is shown, the gauge calibration constant cancels out in (2). Therefore, assuming BAG linearity, (2) yields absolute speed results. However, in order to place the speed vs. pressure data correctly on the speed-pressure plane, the absolute pressure at the pump inlet must be known.

Lastly, a partial pressure gauge (*i.e.*, PPG) is required when making speed measurements of one gas, which in turn causes the desorption of a second gas from a pump. For example, assume that gas species #2 is desorbed from the pump as a consequence of pumping gas species #1. If there is little pumping of desorbed gas #2 by the walls of the dome and associated gauging, then $P_{2H} = P_{2L}$, where P_{2H} is the pressure *above* the aperture and P_{2L} the pressure *below* the aperture, both of desorbed gas #2, and resulting from the pumping of gas #1. Assume now that we introduce gas #1, and that a total-pressure gauge appended the dome has the same sensitivity for both gases. Then, if P_{1H} and P_{1L} are high and low pressures, respectively, of the introduced gas, the indicated speed of the pump, S_i , would be:

$$S_i = C_a \frac{((P_{1H} + P_{2H}) - (P_{1L} + P_{2L}))}{(P_{1L} + P_{2L})}$$

$$S_i = C_a \frac{(P_{1H} - P_{1L})}{(P_{1L} + P_{2L})} \quad (3)$$

We see that the indicated speed is in error as the consequence of the presence of the P_{2L} component in the denominator of (3); ergo, PPGs must be used to discern species when using (2), and when using any multi-gauge speed dome.

TYPES OF PUMPS TESTED

Five pump configurations were tested for He capacity. Table 1 lists some of the salient pump design parameters. To qualitatively size the respective pumps, nitrogen pumping speed measurements were taken subsequent to the He measurements. The *projected cathode area* noted to the right of this table corresponds to the area of the cathodes immediately adjacent to the respective anode assemblies. This includes the area under the pseudo-cells formed by the nesting of the anode cylinders.

Table 1. Pump configurations for which helium capacity was measured.

| TYPE PUMP | N ₂ SPEED L/sec. | CATHODE MATERIAL | NO. OF CELLS | CELL LENGTH mm | CELL DIAM. mm | PROJECTED CATHODE AREA-cm ² |
|--|-----------------------------|------------------|--------------|----------------|---------------|--|
| DIODE, STD. 80 L/sec ¹ | 39 ² | Ti/Ti | 64 | 14.4 | 17.8 | 464 |
| DIODE, DI [®] 80 L/sec ¹ | 36 ³ | Ta/Ti | 64 | 14.4 | 17.8 | 464 |
| TRIODE, StarCell [®] 120 L/sec | 79 ⁴ | Ti/Ti | 106 | 25.4 | 19.8 | 835 |
| DIODE, STD. 110 L/sec | 140 ⁵ | Al/Al | 126 | 25.4 | 20.3 | 1176 |
| DIODE, STD. 270 L/sec | ND | Ti/Ti | 126 | 35.6 | 30.7 | 2186 |

NOTES: 1) Enlarged pump aperture, w/ 203 mm ConFlat[®] flange to match CERN dome.

2) Speed measured @ 3×10^{-7} Torr after pumping 1.8 Torr-L N₂.

3) Speed measured @ 4×10^{-7} Torr after pumping 0.33 Torr-L N₂.

4) Speed measured @ 2×10^{-7} Torr after pumping 0.19 Torr-L N₂.

5) Speed measured @ 1×10^{-7} Torr after 4 hrs. elapsed time; speed w/ Ti/Ti cathodes and under similar conditions, was ~110 L/sec.

The pumps tested included: i) conventional diode configurations, including a standard 80 L/sec and 270 L/sec pump with Ti cathodes, and a 110 L/sec pump with Al cathodes; ii) a DI[®] diode pump with Ta and Ti cathode pairs; and, a StarCell[®] triode pump. The DI[®] diode pump, standard 80 L/sec diode - identical to the DI[®] diode but with Ti cathodes - and the StarCell[®] triode pumps were all new at time of He testing. The other pumps had varied histories of pumping different gas species under UHV conditions. Specifically, the 270 L/sec pump had been used to pump ~100 Torr-L of H₂ and the diode with Al cathodes had been used to pump ~15.2 Torr-L of H₂ prior to the He tests.

HELIUM CAPACITY OBSERVATIONS AND DISCUSSION

At each He measurement, a given amount of gas was introduced into the pump. At the conclusion of the introduction of each prescribed dose of gas, the variable leak was turned off, and the pump absolute He pressure monitored ~20 hours after removing the leak. The gas introduction system was rough pumped with a turbomolecular system subsequent to each sequence of measurements. This afforded assurance that the measured pump base pressures stemmed only from gas backstreaming from the sputter-ion pumps, rather than, in part, from a possibly faulty variable leak.

Helium capacity results for four of the five configurations are given in Fig. 5, where results of He speed measurements for all five pumps are given in Table 2. (The diode with Al cathodes pumped ~3.4 Torr- μ of He prior to pressure run-away. Sequential He base pressure measurements were not made with this pump.)

Results of these measurements suggest: 1) There is little if any difference between a standard diode pump and that of a DI[®] diode in either pump speed or capacity for He. This is not the case for the heavier inert gases such as Ar. In this case, the speed of the DI[®] diode is ~x20 greater than that of a standard diode. This is because much of the kinetic energy of the neutral Ar atom is preserved on reflection from the Ta cathode (i.e., 40-100% of the energy of the incident ion with Ta cathodes; but, 0.8 - 100% from Ti cathodes).⁽¹⁰⁾ Therefore, the neutrals are thereafter more effectively buried in pump elements when originating from Ta cathodes. In the case of He, the possible energies of reflected neutrals of this gas off of Ti and Ta cathodes will be 72-100% and 92-100%, respectively, of the primary ion energy. Therefore, there is no advantage in the use of either type of pump in the pumping of He.

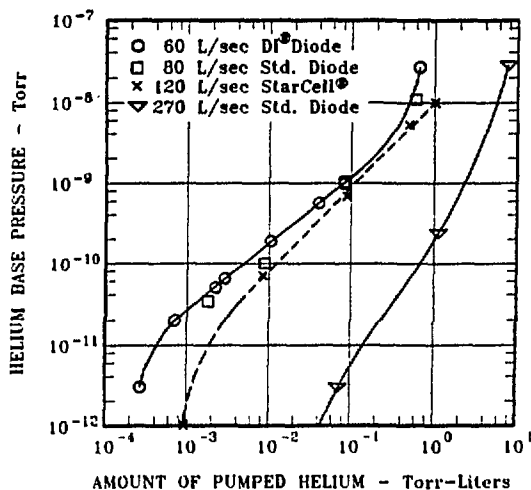


Figure 5. Helium base pressure of various pumps ~20 hours subsequent to the pumping of controlled amounts of helium.

Table 2. Helium pumping speeds and a function of quantity of pressure and helium pumped by a variety of sputter-ion pumps.

| TYPE PUMP | HELIUM SPEED | | HELIUM PRESSURE Torr | ∫ Qdt He Torr-L |
|--|--------------|----------------------|----------------------|-----------------------|
| | L/sec | σ | | |
| DIODE, STANDARD 80 L/sec | 12.2 | 0.2 | 1.2×10^{-8} | 1.78×10^{-3} |
| | 18.3 | 1.8 | 2.1×10^{-7} | 0.0814 |
| | 14.7 | 0.2 | 8.0×10^{-7} | 0.226 |
| | 7.6 | neg | 2.4×10^{-8} | 0.514 |
| DIODE, DI [⊕] 60 L/sec | 12.6 | 0.8 | 3.5×10^{-9} | 7.03×10^{-4} |
| | 14.4 | 1.3 | 3.0×10^{-8} | 0.0824 |
| | 7.0 | 0.4 | 1.2×10^{-7} | 0.661 |
| TRIODE, StarCell [⊕] 120 L/sec | 13.5 | 1.0 | 1.7×10^{-8} | 9.28×10^{-4} |
| | 13.5 | 1.0 | 2.9×10^{-8} | 8.33×10^{-3} |
| | 25.5 | neg | 1.6×10^{-7} | 0.0880 |
| | 28.1 | 0.7 | 1.2×10^{-6} | 0.486 |
| | 23.4 | 0.7 | 1.2×10^{-6} | 1.000 |
| DIODE, STANDARD 110 L/sec w/ Al CATHODES | 51.0 | 9.0 | 2.4×10^{-6} | 5.00×10^{-3} |
| | 35.3 | 12.0 | 4.0×10^{-6} | 0.015 |
| | 51.6 | 1.2 | 1.2×10^{-7} | 0.050 |
| | 36.2 | 1.0 | 3.0×10^{-7} | 0.557 |
| | 27.7 | 1.9 | 5.0×10^{-8} | 0.866 |
| | 8.2 | 0.7 | 2.0×10^{-6} | 1.132 |
| | 13.5 | 0.7 | 2.1×10^{-7} | 1.538 |
| | 19.9 | 1.0 | 2.6×10^{-7} | 1.749 |
| 4.8 | ND | 6.1×10^{-7} | 2.451 | |
| DIODE, STANDARD 270 L/sec | 57.0 | 3.0 | 1.3×10^{-8} | 1.13×10^{-3} |
| | 79.0 | neg | 5.9×10^{-7} | 1.120 |
| | 98.0 | neg | 5.0×10^{-7} | 6.835 |
| | 10.0 | 1.5 | 1.0×10^{-8} | 7.700 |

2) The base pressures of a pump at low pressures and subsequent to pumping He, depend on pump I/P considerations as well as simple cathode/anode ion and neutral implant considerations. This is demonstrated when comparing He data of the 80 L/sec standard and 60 L/sec DI[⊕] diodes with that of the 270 L/sec diode. The arguments for this are as follows: i) The pump's I/P characteristics are proportional to the electrical discharge intensity or space charge stored in the anode cells. This space charge has been shown by Jepsen to depend on the length of the Penning cell.⁽¹¹⁾ Using a simple model, it can be shown that at high pressures the relative amounts of space charge in the two types of pumps is ~14:1, in favor of the 270 L/sec pump;⁽¹²⁾ ii) as will be shown, ~5% of the H₂ pumped by an SIP will be buried as fast neutrals in the anodes of the pump if the anodes can accommodate same. This implies that the area of the anodes plays a secondary role in the neutral implant pumping capacity for He (This is not the case when pumping chemically active gases which afford high cathode sputter-yields.); iii) lacking significant diffusion in the cathodes, He cathode accommodation should be proportional to the implant density, or cathode surface areas; iv) therefore, the product of cathode surface area times the I/P characteristics of the pump is a qualitative measure of the capacity (i.e., base pressure); v) the proportionately higher apparent He capacity of the 270 L/sec pump at very

low pressures stems from the much higher I/P characteristics of this pump at low pressures due to the larger anode cell diameter and length.⁽¹³⁾

3) The triode pump appears to have a proportionately lower capacity for He with higher He charges. However, this pump did not evidence a capacity curve inflection point at higher doses of He. Additional data would have been worthwhile.

REGENERATION AFTER PUMPING HELIUM

We limited pump regeneration experiments to the 60 μ /sec DI[®] diode, 80 μ /sec standard diode and the StarCell[®] triode pump. As a qualitative measure of the success of a regeneration process we measured He desorption pressures as a consequence of pumping N₂ subsequent to each regeneration process. A similar criterion was used by Brothers.⁽³⁾ However, Brothers used H₂ as the He desorption medium in a 500 μ /sec DI[®] pump. The low sputter yield of H₂ ions (*i.e.*, ~ 0.01 for 7.0 keV H₂⁺ ions⁽¹⁴⁾) would lead to significantly less desorption of He on pumping the former gas.

Table 3. summarizes some of the salient observations made regarding the three pumps. The first data entry relating to each pump is the He base pressure of that pump subsequent to the termination of the respective He capacity tests, the elapsed time before the pressure measurement and the amount of He pumped prior to the pressure measurement.

Ideally, one would have preferred to use the same, optimum regeneration procedure with all the pumps. Of course the optimum regeneration process becomes evident after the experiments are conducted. But, we were sailing in uncharted waters with these tests.

The regeneration used with the DI[®] diode pump amounted to a 48 hr., 300°C bakeout on itself. This is tantamount to the pump *stewing in its own juices* over this period. Also, as will be discussed, both ions and neutrals of all gases become buried in the stn. stl. walls of the pump when the pump is energized during normal operation or bakeout. This gas subsequently evolves into the system and impacts on its base pressure. This will be shown to be a significant effect when H₂ pumping with all types of SIPs.

The regeneration of the standard 80 μ /sec diode amounted to a 16 hr. bake of the pump on itself, at 275°C. While at 275°C and energized, the pump was then pumped with a turbomolecular pump (*i.e.*, turbopump) for two hours. After this, N₂ was introduced into the SIP to a pressure of $\sim 3 \times 10^{-5}$ Torr. The pump was left energized (*i.e.*, ~ 200 Wt.) for 7.5 minutes, and then turned off, on and off for five cycles of a period of 10 minutes each. After this, the N₂ leak and bakeout oven were turned off and the turbopump valved out. The pump was then energized.

Table 3. Helium desorption in sputter-ion pumps as a consequence of pumping nitrogen before & after various regeneration techniques.

| TYPE PUMP | HELIUM PRESSURE Torr | NITROGEN PRESSURE Torr | ∫ Qdt N ₂ Torr-L | HOURS AFTER TEST | COMMENTS |
|--------------------------------|------------------------------------|------------------------|-----------------------------|--|--|
| DIODE, DI® 80 L/sec | 2.7 x 10 ⁻⁸ | - | - | 20 | AFTER PUMPING 0.661 Torr-L He. |
| | 4.0 x 10 ⁻¹⁰ | - | - | 64 | AFTER 48 hr., 300°C BAKEOUT. |
| | 1.0 x 10 ⁻⁹ | 3.2 x 10 ⁻⁸ | ~0 | - | INITIAL INTRODUCTION OF N ₂ . |
| | 4.5 x 10 ⁻⁸ | 2.4 x 10 ⁻⁶ | 0.13 | - | CONTINUATION OF N ₂ PUMPING. |
| | 9.5 x 10 ⁻¹⁰ | - | 0.13 | 19 | AFTER TERMINATION OF N ₂ PUMPING. |
| | 1.1 x 10 ⁻⁷ | 2.1 x 10 ⁻⁷ | ~0.13 | - | CONTINUATION OF N ₂ PUMPING. |
| | 3.8 x 10 ⁻⁷ | 4.0 x 10 ⁻⁷ | 0.33 | - | " " N ₂ " |
| | 1.6 x 10 ⁻⁹ | - | 0.33 | 18.5 | AFTER TERMINATION OF N ₂ PUMPING. |
| | 2.5 x 10 ⁻⁸ | 1.3 x 10 ⁻⁸ | ~0.33* | - | CONTINUATION OF N ₂ PUMPING. |
| * See Fig. 6 → { | 2.8 x 10 ⁻⁶ | 1.8 x 10 ⁻⁶ | 1.00* | - | " " N ₂ " |
| | 8.0 x 10 ⁻¹⁰ | - | 1.00 | 20.5 | AFTER TERMINATION OF N ₂ PUMPING. |
| DIODE, STANDARD 80 L/sec | 1.1 x 10 ⁻⁸ | - | - | 17.7 | AFTER PUMPING 0.514 Torr-L He. |
| | 1.1 x 10 ⁻⁷ | 5.5 x 10 ⁻⁹ | ~0 | - | INITIAL INTRODUCTION OF N ₂ . |
| | 5.7 x 10 ⁻⁸ | 5.7 x 10 ⁻⁹ | 0.031 | - | CONTINUATION OF N ₂ PUMPING. |
| | 3.7 x 10 ⁻⁷ | 1.7 x 10 ⁻⁷ | 0.048 | - | " " N ₂ " |
| | 6.0 x 10 ⁻⁷ | 2.0 x 10 ⁻⁷ | 0.087 | - | " " N ₂ " |
| | 3.4 x 10 ⁻⁷ | 3.4 x 10 ⁻⁷ | 1.80 | - | " " N ₂ " |
| | 2.7 x 10 ⁻⁶ | 2.3 x 10 ⁻⁶ | 2.26 | - | " " N ₂ " |
| | 2.2 x 10 ⁻⁶ | 2.2 x 10 ⁻⁶ | 2.66 | - | " " N ₂ " |
| | 2.6 x 10 ⁻⁹ | - | 2.66 | 1.0 | AFTER TERMINATION OF N ₂ PUMPING. |
| | 2.1 x 10 ⁻¹¹ | - | 2.66 | 7.9 | AFTER BAKEOUT & GLOW DISCHARGE. |
| | M.D.S. → < 2.6 x 10 ⁻¹⁴ | - | 2.66 | 22.0 | AFTER BAKEOUT & GLOW DISCHARGE. |
| | 5.2 x 10 ⁻¹⁰ | 9.2 x 10 ⁻⁹ | ~2.66 | - | CONTINUATION OF N ₂ PUMPING. |
| | 8.5 x 10 ⁻¹⁰ | 8.5 x 10 ⁻⁹ | 2.74 | - | " " N ₂ " |
| | 3.2 x 10 ⁻⁹ | 4.2 x 10 ⁻⁸ | 2.78 | - | " " N ₂ " |
| | 4.4 x 10 ⁻⁹ | 4.3 x 10 ⁻⁸ | 2.84 | - | " " N ₂ " |
| | 9.9 x 10 ⁻⁹ | 1.2 x 10 ⁻⁷ | 2.88 | - | " " N ₂ " |
| | 2.0 x 10 ⁻⁶ | 1.4 x 10 ⁻⁷ | 3.02 | - | " " N ₂ " |
| 5.7 x 10 ⁻⁷ | 1.8 x 10 ⁻⁶ | 3.24 | - | " " N ₂ " | |
| 9.6 x 10 ⁻⁷ | 2.4 x 10 ⁻⁶ | 3.73 | - | END OF N ₂ PUMPING; NO MORE DATA. | |
| TRIODE, StarCell® 120 L/sec | 9.8 x 10 ⁻⁹ | - | - | 19.7 | AFTER PUMPING 1.00 Torr-L He. |
| | 1.6 x 10 ⁻⁸ | 7.9 x 10 ⁻⁹ | ~0 | - | INITIAL INTRODUCTION OF N ₂ . |
| | 3.7 x 10 ⁻⁸ | 9.1 x 10 ⁻⁹ | 0.005 | - | CONTINUATION OF N ₂ PUMPING. |
| | 2.0 x 10 ⁻⁸ | 8.6 x 10 ⁻⁹ | 0.010 | - | " " N ₂ " |
| | 1.6 x 10 ⁻⁷ | 1.9 x 10 ⁻⁷ | 0.020 | - | " " N ₂ " |
| | 1.3 x 10 ⁻⁷ | 1.9 x 10 ⁻⁷ | 0.190 | - | " " N ₂ " |
| | ND | 2.0 x 10 ⁻⁶ | 0.190 | - | PRESSURE RUN-AWAY. |
| | 1.3 x 10 ⁻⁶ | 1.8 x 10 ⁻⁶ | 0.266 | - | CONTINUATION OF N ₂ PUMPING. |
| | 2.3 x 10 ⁻⁶ | 2.6 x 10 ⁻⁶ | 1.220 | - | " " N ₂ " |
| | 2.9 x 10 ⁻⁹ | - | 1.220 | 63.7 | AFTER TERMINATION OF N ₂ PUMPING. |
| | M.D.S. → < 2.6 x 10 ⁻¹⁴ | - | 1.220 | 13.5 | AFTER BAKEOUT & GLOW DISCHARGE. |
| | 4.1 x 10 ⁻¹⁰ | 2.1 x 10 ⁻⁶ | ~1.220 | - | CONTINUATION OF N ₂ PUMPING. |
| | 4.1 x 10 ⁻¹⁰ | 2.0 x 10 ⁻⁶ | 1.270 | - | " " N ₂ " |
| | 3.3 x 10 ⁻⁹ | 1.5 x 10 ⁻⁷ | ~1.270 | - | " " N ₂ " |
| | 5.3 x 10 ⁻⁹ | 1.4 x 10 ⁻⁷ | 1.440 | - | " " N ₂ " |
| 4.6 x 10 ⁻⁸ | 1.3 x 10 ⁻⁶ | ~1.440* | - | " " N ₂ " | |
| 3.4 x 10 ⁻⁷ | 1.7 x 10 ⁻⁶ | 2.140* | - | GRADUAL He PRESSURE INCREASE. | |
| 3.8 x 10 ⁻¹⁰ | - | 2.140 | 17.0 | AFTER TERMINATION OF N ₂ PUMPING. | |
| * See Fig. 6 → { | | | | | |
| | | | | | |

The StarCell® triode pump was regenerated as follows: the pump, with high voltage off, was baked at 300°C for 28 hours into a turbopump. After this, and with the pump still at temperature, N₂ was introduced into the pump at a pressure of 5×10^{-5} Torr. The pump SIP was then turned on. The initial power drawn by the pump was ~300 Wt. Due to power supply interlock control provisions, the input power decreased to ~30 Wt. in 30 sec. The high voltage was then turned off for 2-3 minutes. This process was repeated for 50 minutes. Each time the pump was turned back on the duration of glow discharge cleaning became longer, the last on-cycle lasting about five minutes. Thereafter the N₂ leak was turned off, the high voltage turned on and the turbopump was valved out. Three hours later the bakeout oven was turned off.

Helium base pressures of the pumps were measured several hours after the regeneration. As shown in Table 3., the two pumps which were glow discharge regenerated evidenced subsequent He base pressures many orders in magnitude lower than the pump which was not glow discharge cleaned.

The post regeneration pumping of N₂ with all pumps is observed, as noted in Table 3., to cause a significant increase in He pump pressure during and after N₂ pumping. After pumping comparable amounts of N₂ subsequent to regeneration, the base pressure of the DI® diode pump is seen to be ~x20 greater than that of the StarCell® pump. This is probably more attributable to the nature of the regeneration process than the type of pump. That is, the triode pump was deenergized and baked into a turbopump, as well as being glow discharge regenerated with augmented pumping. The DI® diode was merely baked on itself. Also, He which is buried as neutrals in the walls of a triode pump will not be subsequently sputter-desorbed by N₂ ions. The post N₂ series, He base pressure of the standard diode was not measured.

With all three pumps, protracted N₂ pumping at near-constant pressures resulted in the gradual increase in pump He pressure in time (e.g., see Fig. 6). This effect is understandably exaggerated when pumping He in an unregenerated pump.

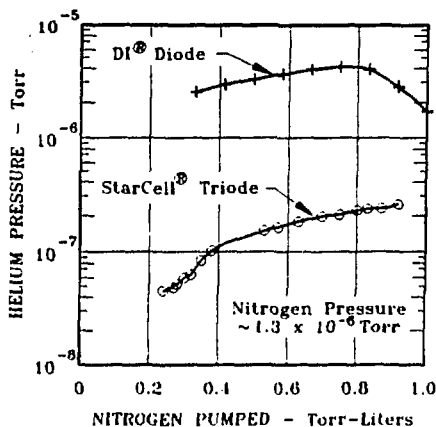


Figure 6. Helium partial pressure subsequent to pump regeneration and as a consequence of pumping nitrogen.

The same effect was observed for H₂ when subsequently pumping He with the 110 z/sec diode pump with Al cathodes. This pump, when having Ti anodes, was first used to pump >15 Torr-z of H₂. The ratio of H₂:He pressure when subsequently pumping He was always in the range of 0.4:1 to 3.0:1, progressively decaying to the lower ratio at the end of He capacity tests (i.e., ~3.4 Torr-z He at pressure run-away).

In summary, the regeneration of pumps subsequent to the pumping of He is seen to be of very modest benefit. The He base pressure several hours after regeneration is a misleading criterion for quantifying the efficacy of regeneration. In the case of the standard diode pump, when operated at a N₂ pressure of $\sim 2 \times 10^{-6}$ Torr, He pressure was reduced by only ~ 2.5 as a consequence of regeneration. Even the triode pump, which underwent a rather severe regeneration process, evidenced only ~ 5 improvement in He pressure on subsequently pumping N₂ at a pressure of $\sim 2 \times 10^{-6}$ Torr. Lastly, the benefits gained by regeneration of the pumps after the pumping of substantive quantities of He seem to be negated with the *subsequent* pumping of a second gas. That is, after removing the N₂ leak, the He base pressures were subsequently higher.

IMPLANTATION OF GAS IN PUMP WALLS

Subsequent to the He capacity measurement made with the 270 z/sec standard diode, the pump elements were replaced with new, special elements with Ti anodes. The pump had not been baked subsequent to the He capacity measurements and installation of these new elements. The pump, with new elements, was installed on the CERN dome, leak checked and then baked for 64 hr. at 300°C into a turbopump. A pump electrical shorting problem occurred while at temperature toward the end of the bakeout cycle. Subsequent to cooldown the short within the pump was remedied, the dome installed and a second leak check attempted. The pump body and internal parts were still at a temperature of $\sim 50^\circ\text{C}$ at this time. The background He in the pump made it impossible to execute a high sensitive leak check. The system was baked at a temperature of 250°C overnight, again into the turbopump. Using the a calibrated leak detector connected to the foreline of the turbopump, we measured a He outgassing rate from the pump of $\sim 2 \times 10^{-7}$ Torr-z/sec. If we assume that the He outgassing rate during the 300°C bake was twice this number, and calculate the total $\int Qdt$ of He stemming from both bakeouts, we conclude that ~ 0.1 Torr-z of He was desorbed from the stn. stl. walls of the pump during bakeout. Therefore, of the 7.7 Torr-z He previously pumped with this pump, we can only conclude that $\sim 1.3\%$ of this gas was implanted as He neutrals and ions in the stn. stl. pump body. We are led by this result to some very interesting conclusions regarding H₂ implantation during normal operation and high temperature bakeouts of an energized pump.

HYDROGEN PUMPING BY SPUTTER-ION PUMPS

The RHIC requires warm-bore H₂ pressures of the order of 10⁻¹⁰ Torr. Assuming a speed ~100 l/sec for these pumps and an operating pressure of 2 × 10⁻¹⁰ Torr, ~6 Torr-l of H₂ will be pumped by the SIPs over a ten year period. However, for hereto-fore inexplicable reasons, the pumping speed of SIPs at these pressures seems negligible. That is, as first pointed out by Singleton, there is a departure in the correlation between pump speed and I/P values at very low pressures.⁽¹⁵⁻¹⁷⁾ Because of the *fussing around* and hidden transactions associated with the use of TSP pumps in combination with SIPs, there is motivation for the exclusive use of SIPs, perhaps augmented with NEG cartridges, in pumping the RHIC warm-bore sections.

A comprehensive treatment of the pumping of H₂ by sputter-ion pumps is given elsewhere.⁽¹⁸⁾ Hydrogen capacity and throughput limits of standard diode SIPs with Ti and Ti-alloy cathodes was reported elsewhere,⁽¹⁹⁾ and the physical processes of H₂ implantation and diffusion in various cathode materials were quantitatively reviewed at a later date.⁽¹⁸⁾ It is shown that H₂ speeds of an SIP at high pressures are dependent on the relative diffusivities of H₂ in the cathodes. Pumps comprising cathode materials with hydrogen diffusivities ranging from ~4.3 × 10⁻¹² to 2.8 × 10⁻⁷ cm²/sec were explored.

The present work started about three years ago. Dr. Derek Lowenstein, the Brookhaven AGS Department Head, found an article published in an obscure journal which extolled the virtues of the use of Al cathodes in SIPs. Because of argon pumping instabilities in LINAC SIPs, we had just incurred great expense for Ta to convert 30% of these pumps to DI[®] diodes. DI[®] diodes, as triode pumps, stably pump substantive quantities of argon. We were asked: "Why not use Al cathodes in these pumps?" We had reservations about H₂ pumping with Al cathodes.

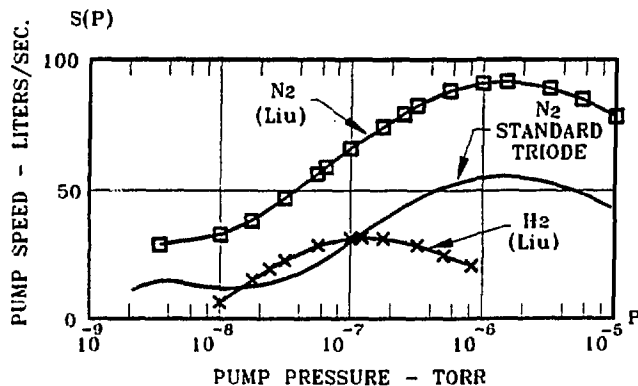


Figure 7.0. Nitrogen speed for a conventional triode sputter-ion pump and nitrogen and hydrogen speed for a triode pump with grided aluminum cathodes (Liu).⁽¹⁹⁾

About this same time Liu and his colleagues reported on the stable pumping of gases, including H₂, with a triode with Al cathodes.⁽²⁰⁾ Liu's results are shown in Fig. 7. The H₂ speed data were reported as taken under *saturated* conditions. The H₂ results were very puzzling as the relative solubilities for H₂ in the metals Al:stn.stl.:Ti are ~1:10⁶:10¹².⁽²¹⁾ From this we speculated that the pumping of H₂ in the triode pump resulted from the burial of neutral hydrogen in the stn. stl. walls of the triode pump.

Therefore, the logic of the low pressure H₂ experiments progressed as follows: 1) Determine if sustained pumping exists for H₂ in a diode with Al cathodes and stn. stl. anodes. 2) If the H₂ capacity is exceeded under these conditions, determine the effect on H₂ capacity stemming from making the anodes out of Ti. 3) If noble gases are buried in the stn. stl. anodes of a pump,⁽²²⁾ would not H₂ also be buried in these anodes? 4) If H₂ is buried in substantive quantities in the Ti anodes, then sustained H₂ pumping should occur even after the Al cathodes are saturated. 5) If substantive quantities of He are buried in the stn. stl. walls of a pump (e.g., the 270 μ /sec diode), and noble gases are substantively pumped in the anodes of a pump, then substituting Ti or Ti-alloys for these members should result in a decrease in H₂ base pressure subsequent to the pumping of H₂. Therefore, the base pressures of pumps in which these materials were substituted should be lower after high pressure H₂ capacity tests or subsequent to a high temperature pump bakeout, with the pump energized, than with pumps not so equipped. Also, low pressure speeds for H₂ should be sustained even after the pumping of H₂ at high pressures.

PUMPS WITH ALUMINUM CATHODES

It was erroneously reported by the principle author that the capacity of the 110 μ /sec diode, noted in Tables 1 and 2, and featuring stn. stl. anodes, was exceeded after pumping \leq 0.19 Torr- μ of H₂.⁽²³⁾ This result seemed absurd in light of work reported by Singleton wherein he concluded that the H₂ capacity of a single-cell pump with Al cathodes was of the order of $\sim 10^{-2}$ Torr- μ /cm².⁽¹⁵⁾ This would put the upper limit of H₂ capacity of the 110 μ /sec pump at ~ 10 Torr- μ .

We revisited our previous H₂ test data. The gas introduction system did not exist at the time of the former H₂ measurements. Because of this, we used steady-state speed results to predict the amount of H₂ pumped prior to exceeding the H₂ capacity of the 110 μ /sec pump with Al cathodes and stn. stl. anodes. It was subsequently determined that the total amount of H₂ pumped, including the initial transient, and somewhat unstable high speed results, was of the order of 2-4 Torr- μ of H₂ at the time of pressure run-away.

We subsequently extended the tests, previously reported on, with the 110 μ /sec pump with Al cathodes and Ti anodes.⁽²³⁾ These final results are shown in Fig. 8. After pumping ~ 15.2 Torr- μ of H₂, the speed of this pump remained a steady-state 6.6 μ /sec for H₂. Tests were ended because we needed the CERN dome for other measurements. Had we used Ti cathodes the

speed of this pump for H₂ would have been of the order of 120 μ /sec. Therefore, we conclude that at least 5% of the H₂ ions impinging on the cathodes must be reflected from these cathodes as neutrals; that is, in order to accommodate the equivalent of 6.6 μ /sec pumping in the pump with Ti anodes.

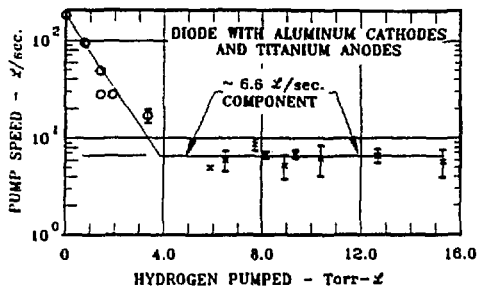


Figure 8. Hydrogen pumping speed of a diode sputter-ion pump with aluminum cathodes and titanium anodes.

The He capacity measurements were made with this same pump after pumping the 15.2 Torr- μ of H₂. At this time it was determined that the capacity of this pump for He was \sim 3.4 Torr- μ at \sim 10⁻⁶ Torr, prior to pressure runaway. Because of the very low hydrogen solubility in Al, it seems reasonable to expect pumps with Al cathodes to have similar capacities for H₂ and He. Results suggest that this is the case.

From the above results we conclude that pumps with Al cathodes have a very limited capacity for the pumping of H₂. We further conclude that substantive quantities of H₂ and H neutrals are buried in the anodes of an SIP. We speculate that this may be one of the reasons for the disparity in SIP I/P results and H₂ speeds at very low pressures. We propose that Liu's steady-state H₂ pumping results, with the triode pump with Al cathodes, stemmed from neutral burial of hydrogen in the pump walls. However, we verified Liu's results for the steady-state pumping of N₂ with Al cathodes (*i.e.*, N₂ speeds were observed to be greater than noted with pumps with Ti cathodes). Also, we noted a steady-state CO pumping speed, with the same Al cathodes, of \sim 110 μ /sec at \sim 3.5 \times 10⁻⁶ Torr after pumping \sim 10 Torr- μ of CO.

STANDARD DIODES WITH TITANIUM ANODES AND CATHODES

Unaware of the He burial effect in the 270 μ /sec diode pump body (*i.e.*, body A, below), we obtained these pumps with stn. stl. and Ti anodes. One of the pump bodies included a port for insertion of a NEG cartridge (body B). Experiments were first conducted on the standard pump with stn. stl. anodes. In each case we baked the pump at 250°C for about 48 hours into a turbopump. Thereafter, at a temperature of \sim 250°C, the SIP was started, turbo pump valved out, and the pump baked on itself for an additional \sim 24 hr. The H₂ base pressure of the system was limited after bakeout by the H₂ speed of the pump and outgassing of the apparatus. All pressure data were taken using the

calibrated QRGAs. Of course, frequent electron multiplier gain measurements were taken, and compensated for in the interpretation of the data.

The series of H₂ measurements included: *i*) system base pressure and pump speed measurements at various times subsequent to the initial system bakeout; *ii*) speed measurements at $\sim 10^{-9}$ Torr; *iii*) speed measurements at higher pressures in the course of pumping fixed quantities of gas; *iv*) system base pressure and speed measurements subsequent to pumping specific quantities of H₂. The elapsed times and quantities of gas pumped in each case were not identical as we took leave from the apparatus from time-to-time. In all but one instance the pumps were operated at 7.0 kV. Speed data were taken at the higher pressures to facilitate determination of absolute speeds of the NEG cartridge as a function of pressure.

Results of the above tests are given in Table 4. Three pump configurations are noted in this table: 1) a standard diode; 2) a standard diode with Ti-alloy anodes and NEG cartridge pump; 3) a standard diode with Ti anodes and with $\sim 80\%$ of the internal pump body shielded from hydrogen ions and reflected neutrals. This latter pump configuration was prompted by the previously mentioned He outgassing effects from a *hot* pump body.

When measuring speeds at the system base pressures, H₂ outgassing of the upper region of the CERN dome served as the source of gas. The outgassing of the upper dome region was determined by measuring the H₂ pressure difference across the dome aperture. In the comments section of Table 4., the total outgassing from the dome is given. This number was arrived at by assuming the total dome outgassing was proportional to the total dome surface area.

The H₂ base pressure of the standard pump, 144 hours after bakeout, was 6.4×10^{-10} Torr. Using the dome outgassing data, we calculate that the speed of the pump is $\sim 40\text{-}60$ z/sec at this pressure. With all pumps, speed data were taken over extended periods. For example, in the case of the standard pump, the first high pressure speed test was conducted at $\sim 2.6 \times 10^{-7}$ Torr. Prior to measuring the reported speed results, ~ 6.6 Torr- z of H₂ was pumped. Thereafter, speed data were taken until ~ 11.9 Torr- z of H₂ was pumped. The leak was then turned off and the gas introduction system evacuated. The pump pumped on the system for 43 hours, at which time the next base pressure measurements were taken. Thereafter, successively greater amounts of H₂ were pumped, etc. In instances where only a few speed datum were taken, the average (*i.e.*, AVG.) of the data are reported. When greater than eight speed datum were taken, the standard deviations of the data were given (*i.e.*, σ of Table 4.). With a value of $\sigma < 5\%$ we reported negligible (*i.e.*, NEG) data spread.

Table 4. Hydrogen base pressures and speeds at various pressures vs. the quantity of hydrogen pumped, for a variety of sputter-ion pump configurations and when augmented with a nonevaporable getter pump.

| TYPE PUMP | HYDROGEN BASE PRESS. Torr | H ₂ PRESS. OF SPEED TEST -Torr | H ₂ SPEED | | ∫ Qdt H ₂ Torr-L | HOURS AFTER TEST | COMMENTS |
|---|---------------------------------|---|----------------------|--------|--------------------------------|--|--|
| | | | L/sec | σ | | | |
| Standard 270 L/sec Diode (Pump Body A) | 6.4 x 10 ⁻¹⁰ | - | ND | - | ~0 | 144 | After 48 hr., 250°C Bakeout. |
| | - | 2.6 x 10 ⁻⁷ | 223 | 35 | 6.6-11.9 | - | |
| | 1.6 x 10 ⁻⁹ | 1.6 x 10 ⁻⁹ | 27 | 3.9 | 11.92 | 43 | Dome Q ~4.0 x 10 ⁻⁸ Torr-L/sec H ₂ . |
| | - | 5.0 x 10 ⁻⁷ | 207 | NEG | 57-74 | - | |
| | 1.1 x 10 ⁻⁹ | 1.1 x 10 ⁻⁹ | 14 | 2.1 | 74.2 | 47 | Dome Q ~2.6 x 10 ⁻⁸ Torr-L/sec H ₂ . |
| | - | 6.0 x 10 ⁻⁶ | 128 | 14 | 81-117 | - | |
| | 1.1 x 10 ⁻⁹ | 1.1 x 10 ⁻⁹ | 17.8 | 1.9 | 117.6 | 42 | Dome Q ~2.6 x 10 ⁻⁸ Torr-L/sec H ₂ . |
| 8.3 x 10 ⁻¹⁰ | 8.3 x 10 ⁻¹⁰ | 19.6 | 3.2 | 159.5 | 48 | Dome Q ~2.6 x 10 ⁻⁸ Torr-L/sec H ₂ . | |
| 1.8 x 10 ⁻⁹ | 1.8 x 10 ⁻⁹ | 21.9 | 4.9 | 159.5 | ~49 | Dome Q ~2.3 x 10 ⁻⁸ Torr-L/sec H ₂ . | |
| Standard 270 L/sec Diode w/ Ti Alloy Anodes & NEG Cartridge (Pump Body B) | 3.3 x 10 ⁻¹⁰ | 3.3 x 10 ⁻¹⁰ | 52 | AVG. | ~0 | ~18 | After B.O. & NEG Regeneration. |
| | 1.4 x 10 ⁻¹⁰ | 1.4 x 10 ⁻¹⁰ | 76 | AVG. | ~0 | 63 | After B.O.; SIP Power off 12 hr. |
| | 2.5 x 10 ⁻¹⁰ | 2.5 x 10 ⁻¹⁰ | 53 | 18 | ~0 | 84 | After B.O.; SIP on ~20 hr. |
| | - | 3.2 x 10 ⁻⁷ | 807 | 29 | 3.3-5.4 | - | Methane, amu 28 & 44 prominent. |
| | 3.3 x 10 ⁻¹⁰ | 3.3 x 10 ⁻¹⁰ | 70 | 14.5 | 5.48 | 18 | Dome Q ~2.8 x 10 ⁻⁸ Torr-L/sec H ₂ . |
| | - | 3.3 x 10 ⁻⁷ | 789 | 14.1 | 21.6-26.1 | - | Methane, amu 28 & 44 prominent. |
| 3.0 x 10 ⁻¹⁰ | ND | ND | ND | 26.59 | ~20 | | |
| Standard 270 L/sec Diode w/ Ti Anodes & ~80% Internal Body Ti Shields (Pump Body A) | 2.5 x 10 ⁻¹⁰ | - | - | - | ~0 | 24 | After 24 hr., 250°C Bakeout. |
| | 2.0 x 10 ⁻¹⁰ | 2.0 x 10 ⁻¹⁰ | 41.3 | AVG. | ~0 | 47 | |
| | - | 2.9 x 10 ⁻⁹ | 136 | 4.8 | 0.004 | - | |
| | - | 1.6 x 10 ⁻⁷ | 165 | 6.7 | ~0.23 | - | |
| | 3.6 x 10 ⁻¹⁰ | 3.6 x 10 ⁻¹⁰ | 28 | AVG. | 0.241 | 14 | Dome Q ~1.7 x 10 ⁻⁸ Torr-L/sec H ₂ . |
| | - | 2.6 x 10 ⁻⁹ | 116.5 | 8.9 | ~0.241 | - | |
| | - | 1.4 x 10 ⁻⁶ | 235 | 10 | 6.3-8.6 | - | |
| | 5.3 x 10 ⁻¹⁰ | 5.3 x 10 ⁻¹⁰ | 28 | 4.5 | 8.65 | 16 | |
| | 4.5 x 10 ⁻¹⁰ | 4.5 x 10 ⁻¹⁰ | 29 | AVG | 8.65 | 39 | Dome Q ~2.1 x 10 ⁻⁸ Torr-L/sec H ₂ . |
| | - | 2.6 x 10 ⁻⁹ | 120 | 12 | ~8.65 | - | |
| | - | 3.0 x 10 ⁻⁶ | 240 | 12 | 55-61 | - | |
| | 5.4 x 10 ⁻¹⁰ | - | - | - | 61.91 | 28 | |
| | 4.0 x 10 ⁻¹⁰ | 4.0 x 10 ⁻¹⁰ | 29.2 | 7.9 | 61.91 | 72 | |
| 4.2 x 10 ⁻¹⁰ | 4.2 x 10 ⁻¹⁰ | 35.0 | NEG. | 61.91 | 96 | Dome Q ~2.5 x 10 ⁻⁸ Torr-L/sec H ₂ . | |
| - | 2.6 x 10 ⁻⁹ | 168 | 16.3 | ~61.91 | - | | |
| 4.3 x 10 ⁻¹⁰ | 4.3 x 10 ⁻¹⁰ | 29 | AVG | ~61.91 | 20 | After 24 hr., 250°C Bakeout. | |

We conclude that there is a gradual deterioration in base pressure of the standard pump as a consequence of pumping successively greater amounts of H₂. There are two subtle and competing effects in this regard. On the one hand, the base pressure of the pump will deteriorate as the consequence of the burial of ions and neutrals in the pump anodes and pump walls. This has the effect of increasing the H₂ outgassing from these members, and thus decreasing the measured speed of the pump. On the other hand, the pumping of significant amounts of H₂ eventually sputter-cleans the surface of the cathodes so that the H₂ pumping efficiency (i.e., pumped H₂ molecules per hydrogen ion impinging on the cathodes) and therefore speed, increases markedly in time.⁽¹⁸⁾ Therefore, the base pressure subsequent to the pumping of substantive quantities of H₂ may or may not be lower than prior to this pumping depending on the two effects. This explains why the base pressure of the pump in the middle of the series of measurements appeared to decrease as a consequence of H₂ pumping (i.e., an increase in pump H₂ speed), where at the conclusion of the experiment, sufficient gas had been buried in the stn. stl. members of the pump to overcome the benefits of increased H₂ speeds.

Subsequent to this test, we conducted a similar series of tests on a pump with Ti-alloy anodes. The results were almost identical to that observed with the first pump. We were puzzled by this result, as we had not yet concluded the extent to which gas was also buried in the pump walls.

The standard pump with Ti anodes, and augmented with a NEG cartridge, was then tested. Due to a fortuitous power shutdown, the NEG cartridge pumped on the entire system and SIP for ~12 hours. After this, we observed a system base pressure of $\sim 1.4 \times 10^{-10}$ Torr. Assuming that the H₂ outgassing from both dome and pump body was of the order of 6×10^{-3} Torr- ℓ /sec, we conclude that the H₂ speed of the NEG at this pressure was of the order of ~ 400 ℓ /sec. The SIP was turned back on and ~25 hrs. later the system base pressure was $\sim 2.5 \times 10^{-10}$ Torr. We speculate that the increase in H₂ pressure may have stemmed from *knock-out* hydrogen liberated from the cathodes by energetic ions. The system base pressure did not seem to deteriorate as a consequence of pumping increased amounts of H₂. However, we noted that the methane family became very pronounced in time. We are not sure if this stemmed from the NEG or from the SIP. Of course, it is known that methane is synthesized by SIPs.⁽²⁴⁾ Also, the NEG surfaces were not shielded from the bombardment of ions or neutrals from the SIP. We will conduct tests in the future to determine if there is some NEG/SIP interaction process going on which supports the creation methane and the other spurious gases noted in these tests.

The final test series involved the use of a standard pump with Ti anodes and with ~80% of the pump body shielded with sheets of Ti. The element pockets were lined with Ti, and the walls of the pump body opposite the elements similarly shielded by leaning sheets of Ti on a diagonal to the foot of the element pockets. This left the top and diagonal portions

of the sides of the pump plenum unshielded with Ti sheet.

Results of these tests indicated the following: 1) The base pressure of the system after bakeout was $\times 2.7$ lower than that of the standard pump. 2) Subsequent to the pumping of substantive quantities of H_2 with the standard and shielded pumps, H_2 speeds in the low 10^{-9} Torr range were $\sim \times 10$ greater with the shielded pump. 3) After pumping ~ 0.24 Torr- ℓ of H_2 with the shielded pump the speed of same was 116 ℓ /sec. This increased to 168 ℓ /sec at the same pressure (i.e., 2.6×10^{-9} Torr) after pumping ~ 62 Torr- ℓ of H_2 . However, the base pressure of the pump deteriorated by $\sim 16\%$. 4) Comparing speeds of the standard and shielded pumps with that of the NEG augmented pump, we conclude that the H_2 speed of the NEG cartridge is ~ 600 ℓ /sec at $\sim 2 \times 10^{-7}$ Torr. Subsequent to pumping comparable quantities of gas, the base pressure of the shielded pump was in all cases $\sim \times 3$ lower in pressure than the unshielded pump.

CONCLUSIONS

1) As the theory predicts, there is little if any difference between a standard diode pump and that of a DI[®] diode in either pump speed or capacity for He. 2) A triode pump of comparable N_2 speed to a standard diode pump appears to have similar capacities for He at very low pressures. However, it appears less effective in the pumping of He at higher He charges. 3) The base pressures of a pump at low pressures and subsequent to pumping He, depend on pump I/P considerations as well as simple cathode, anode and pump body ion and neutral implant considerations. 4) There is no apparent effective manner to regenerate an SIP subsequent to the pumping of He. 5) Helium background pressures, in all SIPs used to pump substantive quantities of He, will gradually increase in time as the result of desorption stemming from the pumping of a second heavier gas. 6) Hydrogen pumped in Al cathodes will be similarly desorbed as a consequence of subsequently pumping He. 7) The He and H_2 capacities of diode pumps with Al cathodes are comparable. 8) Substantive quantities of H_2 , in the form of reflected neutrals, will be pumped in the anodes of an SIP if the anodes are made of Ti or a Ti alloy. 9) Substantiative quantities of ions and neutrals of gases are buried in the walls of all diode SIPs. 10) Neutrals of gases are also buried in the walls of triode SIPs. 11) Shielding the walls of an SIP with Ti and constructing the anodes of this same materials will result in a significant increase in pumping speeds for H_2 at low pressures and thus improve on the base operating pressures. 12) Work is merited to more effectively shield the walls and other st. stl. components of SIPs to improve on low pressure operation.

ACKNOWLEDGEMENTS

We thank Dr. D. Lowenstein for challenging our ideas and making possible the early studies of pumps with Al cathodes. We thank Dr. S. Ozaki the Director of the RHIC Project for supporting the continuation of this work for RHIC applications. Lastly, we thank K.W. Vitkun for his assistance in setting up the equipment and making some of the He capacity measurements.

REFERENCES

- 1) Ozaki, S., "RHIC Project", IEEE Particle Accelerator Conference, Accelerator Science and Technology 5(5), 2901(1991).
- 2) Welch, K.M., Capture Pumping Technology: An Introduction (Pergamon Press, Oxford, 1991), pp. 65-183.
- 3) Brothers, C.F., "Ion Pumping of Large Amounts of Helium", J. Vac. Sci. Technol., 5(6), 208(1968).
- 4) Milleron, N., Reinath, F.S., "Performance of a Six-inch Triode P.I.G. Pump Compared to a Perfect Pump", Transactions of the 9th National American Vacuum Society Symposium, (The Macmillan Company, New York, 1962), p. 356.
- 5) Dallos, A., Steinrisser, F., "Pumping Speeds of Getter-Ion Pumps at Low Pressures", J. Vac. Sci. Technol. 4(1), 6(1967).
- 6) Rozgonyi, G.A., "Increase of Residual Background Gases During Ultrahigh-Vacuum Mass Spectroscopic Analysis", J. Vac. Sci. Technol. 3(4), 187(1966).
- 7) Welch, K.M., Ibid, pp. 72-78.
- 8) Fischer, E., Mommsen, H. "Monte Carlo Computations on Molecular Flow in Pumping Speed Test Domes", Vacuum 17, 309(1967).
- 9) NIST is an acronym for The National Institute of Standards and Technology, formally the National Bureau of Standards.
- 10) Welch, K.M., Ibid, p. 104.
- 11) Jepsen, R.L., "Magnetically Confined Cold-Cathode Gas Discharges at Low Pressures", J. Appl. Phys. 32(12), 2619(1961).
- 12) Welch, K.M., Ibid, Prob. 4, p. 166.
- 13) Rutherford, S.L., "Sputter-Ion Pump for Low Pressure Operation", Proc. 10th Nat. AVS Symp., 1963 (The Macmillan Company, New York, 1964), p. 185.
- 14) KenKnight, C.E., Wehner, G.K., "Sputtering of Metals by Hydrogen Ions", J. Appl. Phys. 35(2), 322,(1964).
- 15) Singleton, J.H., "Hydrogen Pumping by Sputter-ion Pumps and Getter Pumps", J. Vac. Sci. Technol. 4(1), 6(1967).
- 16) Singleton, J.H., "Hydrogen Pumping Speed of Sputter-ion Pumps", J. Vac. Sci. Technol. 6(2), 316(1969).
- 17) Singleton, J.H., "The Performance Characteristics of Modern Vacuum Pumps", J. Phys. E6, 685(1973).
- 18) Welch, K.M., Ibid, pp. 106-124.
- 19) Welch, K.M., "New Developments in Sputter-Ion Pump Configurations", J. Vac. Sci. Technol. 13(1), 498(1976).
- 20) Liu, Y.C., Lin, C.C., Lee, S.F., "Pumping Mechanisms for N₂ Gas in a Triode Ion Pump with Al100 Aluminum Cathodes", J. Vac. Sci. Technol. A6(1), 139(1988).
- 21) Welch, K.M., Capture Pumping Technology: An Introduction

- (Pergamon Press, Oxford, 1991), p. 128.
- 22) Welch, K.M., Ibid, p. 98.
 - 23) Welch, K.M., "Pumping Mechanisms of Sputter-Ion Pumps at Low Pressure Operation", 1991 IEEE Particle Accelerator Conference Transactions, Vol. 4, 2269(1991).
 - 24) Welch, K.M., Ibid, p. 162.